applied sciences

MDPI

Article

Simulation of Parameters of Plasma Dynamics of a Magneto Plasma Compressor

Victor V. Kuzenov [1], Sergei V. Ryzhkov [1,*] and Aleksey Yu. Varaksin [2]

[1] Thermal Physics Department, Bauman Moscow State Technical University, 105005 Moscow, Russia; vik.kuzenov@gmail.com
[2] Joint Institute for High Temperatures, Russian Academy of Sciences, 125412 Moscow, Russia; varaksin_a@mail.ru
* Correspondence: svryzhkov@bmstu.ru; Tel.: +7-(499)-263-6570

Abstract: The main purpose of this article is to study the features of the structure and spectral brightness characteristics of pulsed emitting discharges of the magneto plasma compressor type in dense gases over a wide range of energy–power parameters. A numerical simulation of plasma dynamic magneto plasma compressor discharge in gases is carried out. Different quasi-stationary regimes have been studied and the main characteristics have been estimated.

Keywords: gas discharge; magneto plasma compressor; mathematical model; radiation plasma dynamics; shock wave

check for updates

Citation: Kuzenov, V.V.; Ryzhkov, S.V.; Yu. Varaksin, A. Simulation of Parameters of Plasma Dynamics of a Magneto Plasma Compressor. *Appl. Sci.* **2023**, *13*, 5538. https://doi.org/10.3390/app13095538

Academic Editor: Emilio Martines

Received: 4 April 2023
Revised: 26 April 2023
Accepted: 27 April 2023
Published: 29 April 2023

1. Introduction

Recently, theoretical and experimental studies of non-stationary processes in pulsed radiation magneto gas dynamic systems have been of great interest. Such systems include plasma sources of radiation and shock-wave generators, thermonuclear systems, systems for preliminary electromagnetic acceleration of targets, magneto plasma compressors and plasma accelerators, and pulsed plasma dynamic systems for controlling high-speed gas flows, as well as systems for plasma-stimulated ignition and combustion of fuel mixtures.

The pulse plasma accelerator of the erosion type (magneto plasma compressor (MPC) [1–3]) in a vacuum, operating in self-focusing mode, is an effective device for generating flows of emitting plasma with a density of up to $10^{24} \div 10^{26}$ m^{-3} and a temperature of up to 100 kK and higher. On this basis, technical devices can be created that allow efficient conversion of the electric energy of the storage unit into thermal radiation of the ultraviolet (UV) and vacuum ultraviolet (VUV) range [4–6]. However, since the share of kinetic energy in the total energy balance of open vacuum magneto plasma compressor discharges is large, its thermalization methods are of particular interest: collision of plasma flow with a solid obstacle, counter interaction of high-speed plasma jets, etc. Magneto plasma compressor discharges in air, argon, and other inert gases with initial pressures in the range of $P_0 = 10^3 \div 3 \times 10^5$ Pa at normal temperature $T_0 = 300$ K have been experimentally and theoretically studied in a series of works [7–9].

The MPC parameters: the length of the channel (<1 cm), the main electrode assembly $2R_1 = (0.8 \div 1.5) \times 10^{-2}$ m and external electrode $2R_2 = (3 \div 10) \times 10^{-2}$ m, the capacity C ~ 900 μF, stored energy $W_0 = CU_0^2/2 = 0.3 \div 500$ kJ, the discharge current 5–100 μs, and the amplitude of the current $J_m \approx 100 \div 2000$ kA.

Theoretical and numerical modelling of magneto plasma compressor discharges is a necessary stage of research which allows quantification of the parameters and internal structure of discharge plasma, giving a correct interpretation of the available experimental data, allowing optimization of such multi-parameter systems, and determining the peculiarities of plasma modes and parameters in the areas of energy–power and the structural characteristics of different systems not yet covered by experiments [10–14].

The earlier work of the authors is devoted to the calculation, description, and justification of the mechanisms of energy transfer in the plasma formation of magneto plasma compressor discharges. The main purpose is to study the features of the structure and the spectral brightness characteristics of pulsed radiating discharges of the MPC type in a dense gas over a wide range of energy–power parameters. It should be noted that no optimization of plasma dynamic processes in the magneto plasma compressor discharge was carried out in this research.

2. Model of the MPC Discharge and Numerical Solution Method

The goal of this research is the development of a mathematical model as well suited as possible to the experimental conditions and the systematic numerical study of discharges in gases for a wide range of variation in basic parameters of the magneto plasma compressor and the ambient gas environment based on this model. The plasma formation processes of a magneto plasma compressor discharge in gas are generally three dimensional and some fluctuations are caused both by spatial and temporal inhomogeneity [15–25]. The full model is presented in the literature [12,14,19].

In this paper, 3D effects are not taken into account and the mathematical model of the MPC discharge is presented on the basis of a 2D (axisymmetric) unsteady system of equations of viscous single-temperature radiation plasma dynamics. The term plasma dynamics used in the work implies a physical discipline that includes a mathematical description (in the form of a continuous medium) of plasma dynamics (taking into account the presence of electromagnetic fields and currents within them), radiation transfer processes in plasma (over a wide range of wavelengths), and its interaction with solids (electrodes, walls, etc.).

The equation for the capacity is [26]:

$$\frac{1}{c^2}\frac{dL_C J}{dt} + R_C J = U_k,\ \frac{dU_k}{dt} = -\frac{J}{C}$$

where the conditions in the initial moment of time are $t = 0,\ J = 0,\ U_k(t=0) = U_0$, J—full current; $U_0 = U_k(t=0),\ U_k(t)$—initial and current voltage on the C bank, respectively; $R_C = R_0 + R_{pl} - \frac{1}{2c^2}\frac{dL_{pl}}{dt}$, $L_C = L_0 + L_{pl}$; $L_0,\ R_0$—inductance and resistance of the external circuit; $L_{pl} = \frac{c^2}{4\pi J^2}\int\limits_V H^2 dV$—MPC plasma inductance; $R_{om} = \frac{1}{J^2}\int\limits_V \frac{j^2}{\sigma} dV$, $R_{pl}(t) = \frac{1}{J^2}\int\limits_0^{\ell_k}\int\limits_0^{r_k}\left(\vec{j}\,\vec{E}\right)dV$, $R_{pldyn}(t) = \frac{1}{cJ^2(t)}\int\limits_V \vec{V}\left[\vec{j}\,\vec{H}\right]dV$—respectively, ohmic, plasma, and plasma dynamic resistances of the discharge plasma.

The radiation fields for seven spectral groups are calculated according to:

$$\frac{1}{J}\frac{\partial(Jq_{i\xi})}{\partial\xi} + \frac{1}{J}\frac{\partial\left(Jq_{i\eta}\right)}{\partial\eta} + \chi_i c U_i = 4\chi_i\sigma_i T^4,\ \frac{c}{3}\frac{\partial U_i}{\partial\xi} + \chi_i q_{i\xi} = 0,\ \frac{c}{3}\frac{\partial U_i}{\partial\eta} + \chi_i q_{i\eta} = 0$$

where $U_i(y,z,t)$—the energy density, χ_i—absorption coefficient. Functions of flow limiters are used in the calculations performed [27,28].

The conductivity coefficient λ_Σ and viscosity coefficient μ_Σ [29], the ASTEROID computer system [30], and the Thomas–Fermi model [31] are used for calculations.

In order to solve the radiation transfer equations, the conditions for the absence of radiation incident from the outside were set at the boundaries of the computational domain, and a condition for the symmetry of radiation fluxes was set on the axis of symmetry. In order to determine the magnetic field strength $B_\varphi(r,\ z,\ t)$ at the left boundary of the calculated area Γ, the following relations were used: $B_\varphi = \frac{2Jr}{cr_1^2}$, $r \le r_1$; $B_\varphi = \frac{2J}{cr}, r \in [r_1,\ r_2]$; $B_\varphi = \frac{2J}{cr}\frac{r_3^2 - r^2}{r_3^2 - r_2^2}$, $r \in [r_2,\ r_3]$; $B_\varphi = 0$, $r \in [r_3,\ r_k]$.

The "hyperbolic" ("convective") part of the equations is:

$$\frac{\partial \vec{U}_i}{\partial t} + \frac{\vec{F}\left(\vec{U}_{i+1/2}\right) - \vec{F}\left(\vec{U}_{i-1/2}\right)}{\Delta_\xi} = \vec{F}_r,\ \Delta_\xi = [\xi_{i-1/2} - \xi_i, \xi_{i+1/2} - \xi_i]$$

The reconstructed function $Y(\xi)$, $\xi \in [-\Delta_\xi/2, \Delta_\xi/2]$, is:

$$Y(\xi) = F_i^n(\xi) = R(\xi) + \\ +a_i[\xi-\xi_i]^3 + b_i[\xi-\xi_i]^4 + c_i[\xi-\xi_i]^5 + d_i[\xi-\xi_i]^6 + e_i[\xi-\xi_i]^7 + g_i[\xi-\xi_i]^8 + h_i[\xi-\xi_i]^9$$

A part of the "reconstructed" function at time t^n is determined by an expression of the form:

$$R(\xi) = \\ = \begin{cases} R_T = Y_i + \phi(Y_i)\left(\frac{\partial Y}{\partial \xi}\right)_i[\xi-\xi_i] + \frac{\phi(Y_i)}{2!}\left(\frac{\partial^2 Y}{\partial \xi^2}\right)_i[\xi-\xi_i]^2, & \ell_i \approx 0, \quad \text{для } \xi \in \left[-\frac{\Delta_\xi}{2}, \frac{\Delta_\xi}{2}\right], \\ R_{L-B} = Y_i + \phi(Y_i)\left[f(\xi-\xi_i)p_1 + \frac{f^2(\xi-\xi_i)}{2!}p_2\right], & \ell_i \approx 1, \quad \text{для } \xi \in \left[-\frac{\Delta_\xi}{2}, \frac{\Delta_\xi}{2}\right], \end{cases}$$

These are the first coefficients of the decomposition of the function $Y(\xi)$ into a truncated Burman–Lagrange series [32]. Obviously, the accuracy of the approximation (using the main part $R(\xi)$) of the "reconstructed" function $Y(\xi)$ depends on the order of accuracy (approximation error) of the recovery of the values of the derivatives $(\partial Y/\partial \xi)_i$ and $\left(\partial^2 Y/\partial \xi^2\right)_i$.

The function $Y(\xi)$ satisfies the conditions of smooth conjugation:

$$F_i^n(\xi_{i-1}) = Y_{i-1}^n,\ F_i^n(\xi_{i+1}) = Y_{i+1}^n,\ dF_i^n(\xi_{i-1})/d\xi = Y_{\xi,i-1}^n,\ dF_i^n(\xi_{i+1})/d\xi = Y_{\xi,i+1}^n$$

as well as the condition of conservativeness of the reconstructed function $Y(\xi)$:

$$\frac{1}{\Delta_\xi}\int_{-\frac{\Delta_\xi}{2}}^{+\frac{\Delta_\xi}{2}} Y_i^n(\xi)d\xi = Y(\xi_i)$$

For the reconstructed function $Y(\xi)$, the following relations (Leibniz formula) should be used:

$$\left.\frac{d[W\cdot F_i^n]}{d\xi}\right|_{\xi_{i-1}} = \left[W\cdot Y_{\xi,i-1}^n\right]\Big|_{\xi_{i-1}} + \left[\dot{W}_\xi \cdot Y^n\right]\Big|_{\xi_{i-1}},\ \left.\frac{d[W\cdot F_i^n]}{d\xi}\right|_{\xi_{i+1}} = \left[W\cdot Y_{\xi,i+1}^n\right]\Big|_{\xi_{i+1}} + \left[\dot{W}_\xi \cdot Y^n\right]\Big|_{\xi_{i+1}}$$

where $\dot{W}$—derivative of the W function [32,33]

An adapted computational grid and a curved coordinate system (ξ, η) were created based on the methodology described in [34,35]. The diffusion approximation of the radiation transfer equation was solved in the work using a modification of the alternately triangular method with conjugate gradients [36].

The "hyperbolic" ("convective") parts were tested [32,37] and implemented in a single-diaphragm aerodynamic shock tube of GUAT IPMeh RAS. The other calculations were performed in [34,35,38,39].

3. Electrical Parameters and Power Regimes for Discharge

The most important feature of the electrical efficiency dependence on the average power $\eta_{el}(P_{el1}) = \int_0^{t_1} R_{пл}(t)J^2(t)/W_0 dt$ is a relatively weak influence of P_{el1} (P_{el1}—the average electrical power released in the MPC discharge plasma during the first half-cycle of the current) on η_{el}: an increase in P_{el1} by two orders leads only to an insignificant decrease $(10 \div 15\%)$ η_{el1}, in contrast to discharges with the ohmic mechanism of plasma heating. At identical power parameters of the storage geometry magneto plasma compressor electric efficiency, η_{el} increases (with simultaneous growth of $\overline{R}_{pl} = \frac{1}{t_1}\int\limits_0^{t_1} R_{pl}(t)dt$ (here and further, the sign from above "–" means averaging over time t) and a reduction in the discharge current amplitude) with a decrease in the density ρ_0 of the surrounding gas. Both mentioned facts testify to the manifestation and significant influence on R_{pl} and η_{el} of energy dissipation in the electric discharge systems under consideration.

Ponderomotor forces are the forces acting on plasma in the magnetic and electric field. There is an electromagnetic (ponderomotor) force (for a thin conductor, this expression corresponds to the Bio–Savard law) for plasma generation in the MPC discharge (for the case of magnetic permeability).

The question about the role of energy dissipation in magneto plasma compressor discharges is one of the key ones and needs to be considered independently. The calculated value of effective plasma load resistance can be represented as:

$$R_{pl}(t) = \frac{1}{J^2(t)}\int\limits_V \vec{j}\,\vec{E}\,dV = R_{om}(t) + R_{pldyn}$$

where $R_{om}(t)$ is the value of that part of the total effective resistance, which is associated with the process of ohmic heating of the plasma, $R_{pldyn}(t)$ determines the nature of energy dissipation, caused by processes of transformation of electromagnetic energy into the work of ponderomotive forces, i.e., it is responsible for the plasma dynamic mechanism of plasma heating.

All systematic investigations reveal one dimensionless criterion, the value of the ratio $\lambda_R = \overline{R}_{om}/\overline{R}_{pl}$ will mainly depend on its value. This regime parameter is:

$$A_m = \left(\frac{\overline{p}_m(z = 0,\ t_m)}{\rho_0 D^2}\right)^{1/2}$$

where $\overline{p}_m(z = 0,\ t_m)$ is the pressure of the magnetic field for $(z = 0,\ t_m)$, and $\rho_0 D^2$ is the full velocity of the gas flow coming up onto the shock wave.

As numerical simulations have shown, the average (during the first half-cycle of the current) velocity D of the head shock wave in the axial direction is satisfactorily approximated by the expression:

$$D = K_D\left(\frac{P_{el1}}{\rho_0 \pi r_2^2}\right)^{1/3}$$

where K_D is a relatively weak (~1 for 10^7–10^{10} W, $\rho_0 = 10^{-2}$ kg/m^3) function of P_{el1} and ρ_0. The defining parameter A_m can be written as:

$$A_m = \frac{\mu_0^{1/2}\Gamma_m}{K_D}\left(\frac{J_m^3}{\rho_0^{1/2}P_{el1}}\right)^{1/3}$$

where $\Gamma_m = (\pi r_2)^{1/3} f(r_2/r_1)/\left(2\sqrt{2}\pi r_1\right)$ is the geometric factor.

The A_m values for some typical design variants of the magneto plasma compressor (with internal radius 0.8×10^{-2} m and external radius 5×10^{-2} m) in Ar are presented in Table 1. A generalized interpolation of the dependence λ_R on the parameter A_m, calculated by equation, shown in Figure 1 (icons show some calculated values of the parameters $\lambda_R = \overline{R}_{om}/\overline{R}_{pl}$ and $\lambda_E = \overline{E}_{kin}(t_m)/\overline{E}_{int}(t_m)$).

Table 1. Mode parameter A_m dependent on gas pressure p_0 and parameters of the power storage magneto plasma compressor discharge.

p_0, MPa	C, μF	U_0, kV	W_0, kJ	A_m
10^{-3}	28.6	10 30 50	1.43 12.9 35.7	0.6 0.9 0.93
	750	2 5 10	1.5 9.37 37.5	0.48 0.78 0.91
10^{-2}	28.6	10 30 50	1.43 12.9 35.7	0.3 0.65 0.76
	750	5 10	9.37 37.5	0.6 0.85
10^{-1}	28.6	30 200	12.9 571	0.36 0.95
	750	2 5 10	1.5 9.37 37.5	0.25 0.4 0.54

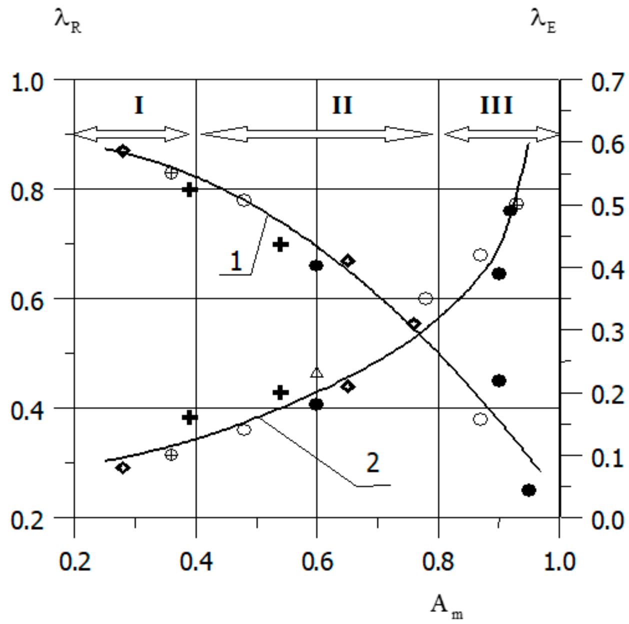

Figure 1. Generalized dependences $\lambda_R = \overline{R}_{om}/\overline{R}_{pl}$ (1) and $\lambda_E = \overline{E}_{kin}(t_m)/\overline{E}_{int}(t_m)$ (2) on parameter A_m (the A_m range corresponds to Table 1). •, ♦, +, ○—Calculation; I—region of ohmic mode parameters; II—region of transition mode parameters; III—region of plasma dynamic mode parameters.

As can be seen, the role of the ohmic energy dissipation mechanism is significant over practically the whole range of power modes of magneto plasma compressor discharge and the surrounding gas densities.

At values of $A_m < 0.3$–0.4, the ohmic resistance share in the total plasma load resistance is the main one ($\lambda_R \geq 0.8$), and therefore it can be argued that the main mechanism of plasma heating in such modes is Joule heating. With an increasing A_m parameter, i.e., an increasing discharge current amplitude J_m and a decreasing gas density ρ_0, a monotonic decrease in λ_R is observed.

For regimes characterized by values of $A_m > 0.8$, the part of ohmic resistance is relatively low ($\lambda_R = 0.2$–0.4), and the plasma dynamic mechanism of plasma heating of the magneto plasma compressor discharge becomes predominant. In the range of A_m = 0.4–0.8, the role of both mechanisms of plasma heating of the magneto plasma compressor discharge is commensurable.

These results show that the value of the A_m parameter essentially defines the mode of IGC discharge plasma heating and, therefore, it can be called a mode parameter. In the region of A_m < 0.3–0.4, there is an ohmic mode of heating; in the region of A_m > 0.8, there is a plasma dynamic mode of heating; and at $A_m \approx$ 0.4–0.8, there is a transitive mode (Figure 1). According to equation, the parameter A_m value depends on the main electric parameters of the discharge circuit and gas density as parameter $A_m \sim (CW_0/\rho_0 L_C)^{1/6}$, and plasma heating mode control can be most effectively achieved by increasing the capacity of power storage C and the initial charging voltage U_0 ($A_m \sim (CU_0)^{1/3}$), as well as by reducing the gas density ρ_0.

As the numerical simulations show, according to the proposed classification, discharges in rarefied spheres (ρ_0 < 0.1 kg/m^3) and a high level of power storage capacity (for C = 28.6 μF: U_0 > 30 kV, C = 750 μF: U_0 > 5 kV) can be attributed to the plasma dynamic modes of plasma heating of magneto plasma compressor discharges. At atmospheric (and higher) pressures (ρ_0 > 1 kg/m^3), the implementation of modes with a significant predominance (λ_R < 0.2–0.3, A_m > 0.8) of the plasma dynamic heating mechanism is only possible at high values of U_0 (for example, for P_0 = 0.1 MPa: at C = 28.6 μF: U_0 > 100 kV; at C = 750 μF: U_0 > 20 kV).

4. Plasma Dynamic Parameters for Discharge in Magneto Plasma Compressor

The performed numerical simulation of erosive magneto plasma compressors has revealed the complex self-consistent nature of the processes of energy transfer from storage to plasma and the processes of erosive plasma formation, the dynamics of acceleration, the interaction of light erosive plasma streams between themselves and the surrounding gas, and, finally, the processes of transformation of energy W_1 dissipated in plasma into internal E_{int} and kinetic E_{kin} energy and into broadband $E_{s\Sigma}$ radiation energy, escaping from discharge plasma into the surrounding gas medium (in the "transparency" window). The character of the energy interconversions of the discharge is connected with the mechanism of energy dissipation of the storage device into plasma load and depends on the mode parameter A_m. The dependence of the ratio of the total kinetic plasma energy $E_{kin}(t_m) = \int\limits_V \left(\rho\left(\vec{V}\right)^2/2\right)dV$ to the total internal energy $E_{int}(t_m) = \int\limits_V edV$ (calculated at the moment of time t_m of the discharge current maximum), i.e., $\lambda_E = E_{kin}(t_m)/E_{int}(t_m)$ from value A_m is presented in Figure 1 (for different energy power modes and densities of ambient gas; calculated values of λ_E are marked).

The approximation curve $\lambda_E(A_m)$ is a monotonically increasing function showing that the fraction of kinetic energy of plasma formation in relation to the internal one increases with the transition of plasma heating mode from an ohmic (λ_E < 0.15, A_m < 0.4) to a plasma dynamic (λ_E = 0.3–0.5, A_m > 0.8) regime. In other words, upon realization of the plasma heating, a significant portion (in the limit of parameters $A_m \to 1$, $\lambda_E \to 1$) of the energy input to the plasma is converted into kinetic energy of the moving erosive plasma and shock-compressed gas (plasma).

In the region of magneto plasma compressor parameters corresponding to the ohmic heating mechanism (A_m < 0.4), the main part of the energy is concentrated into the internal energy of the erosive plasma, the kinetic energy of which is small due to the relative smallness of the accelerating ponderomotive forces. In the transition region where the joint action of ohmic and plasma dynamic regimes is carried out, the parameter $A_m \approx$ 0.4–0.8 and the share of the total kinetic energy of the plasma in relation to the internal one is significant (λ_E = 0.2–0.4).

In more powerful modes (i.e., at high values of discharge current amplitude J_m in the transition regime) and/or at a decrease in ambient gas density ρ_0, the corresponding parameter A_m = 0.4–0.8 (ohmic–transient operation regime for discharge in the magneto plasma compressor).

The strong gas dynamic shock wave in the surrounding gas (SWG) propagation velocity in the near-edge zone is higher than the SWG velocity in the peripheral zone. The transient regime has a shock front axial coordinate in the axial region; its value, by the time of the discharge current maximum, is about the size of the magneto plasma compressor midpoint, i.e., $z_m \approx Dt_m \geq 2r_2$. Velocity lines have shown in Figure 2.

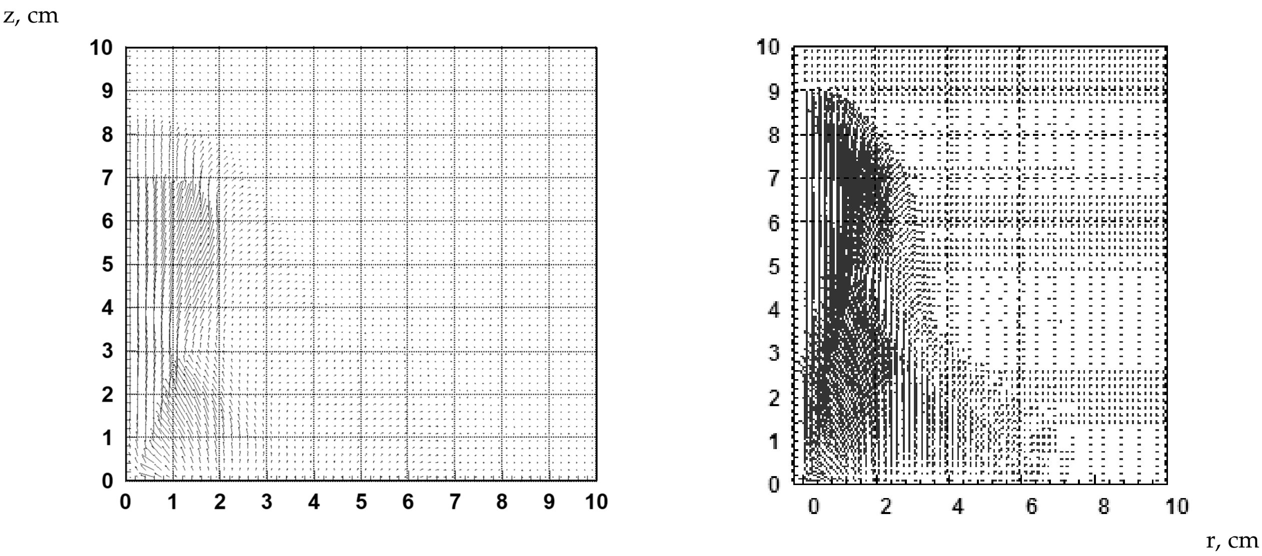

(**a**) (**b**)

Figure 2. Vector velocity field for the magneto plasma compressor (C = 750 µF) in argon: (**a**) U_0 = 5 kV, P = 0.01 MPa, t = 15.3 µs; (**b**) U_0 = 10 kV, P = 0.001 MPa, t = 6.5 µs.

Figure 3 consists of the level lines for density and temperature at discharge current J = 353 kA for the magneto plasma compressor with the parameters C = 750 µF, and U_0 = 10 kV, $R_1 = 0.8 \times 10^{-2}$ m, and $R_2 = 5 \times 10^{-2}$ m for argon.

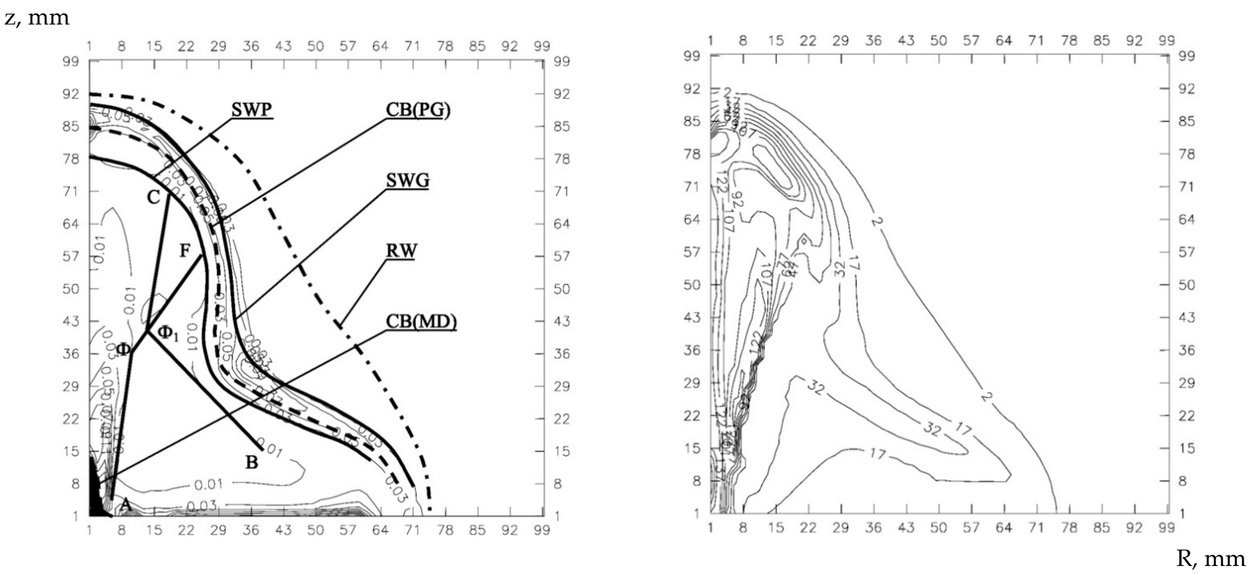

(**a**) (**b**)

Figure 3. Density (kg/m^3) level lines (**a**), temperature (kK) (**b**) for argon, pressure 10^3 Pa, A_m = 0.85: SWP—shock wave in the plasma, CB(PG)—contact boundary, separating the plasma and gas, CB(MD)—contact boundary between metal and dielectric, RW—radiation wave.

Figure 4 contains the level lines for Alfvén velocity (km/s) and velocity modulus (km/s) at current J = 353 kA for the magneto plasma compressor parameters C = 750 µF, and U_0 = 10 kV, $R_1 = 0.8 \times 10^{-2}$ m, and $R_2 = 5 \times 10^{-2}$ m for argon.

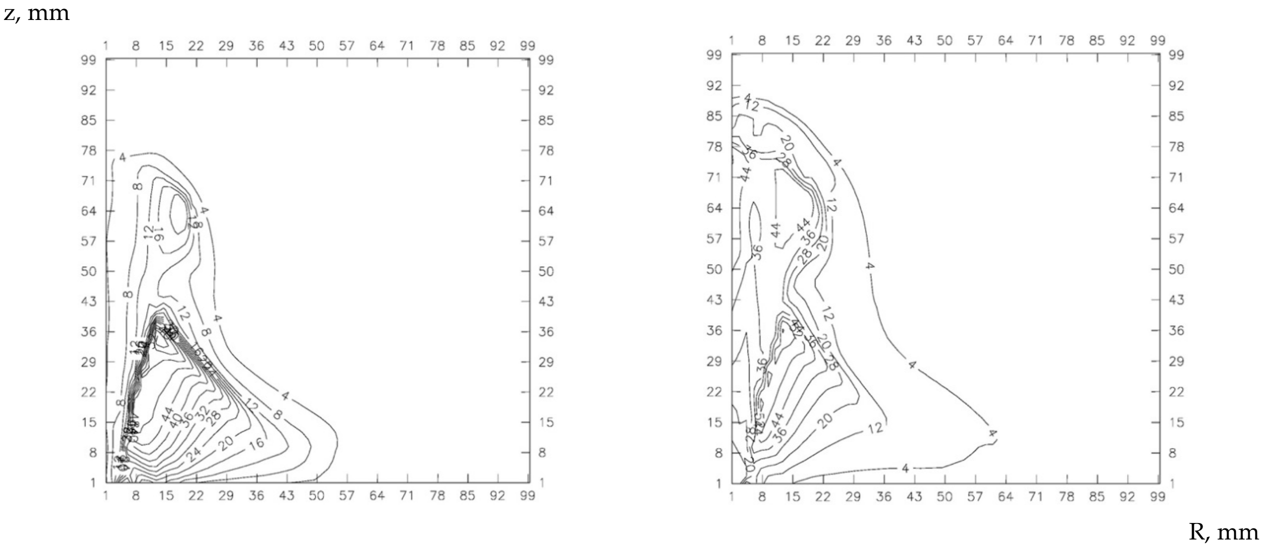

(**a**) (**b**)

Figure 4. The Alfvén velocity lines (**a**), and the velocity modulus (**b**) at time t = 6.5 microseconds for the magneto plasma compressor (internal radius $R_1 = 0.8 \times 10^{-2}$ m, and external radius $R_2 = 5 \times 10^{-2}$ m) with characteristics C = 750 µF, U_0 = 10 kV for Ar.

In the generalized interpolation (according to the results of all calculations), the dependence λ_R value on the A_m parameter shows that the role of the ohmic energy dissipation mechanism is significant over almost the entire range of discharge power regimes in the magneto plasma compressor and the ambient gas densities.

5. Comparison of the Results of Calculations of MPC Discharges in Gases with Experimental Data

The parameters of the device were the following: C = 30–900 µF, U = 2–200 kV, an argon and air environment, p = 0.01–0.25 MPa.

First of all, we note a satisfactory (5–10%) coincidence with the experiment of electrical parameters (amplitudes, degree of attenuation, and duration of half-periods) of the pulses of discharge current and voltage on the electrodes for all of the energy–power modes studied in the experiment.

In order to illustrate what has been said, Figure 5 shows the graphical dependences of the experimental [15,16] and calculated basic electrical parameters of the MPC discharge (C = 750 µF, U = 5 kV) on the density of gas (Ar). Here, the energy is supplied to the plasma in first half-cycle of MPC discharge.

The dynamics of changes in the position of the external boundaries of the discharge over time in all MPC power modes, both in calculations and in experiments, satisfactorily coincide. The dynamics of the changes in the velocity of the head of the shock wave in the gas in the direction of the discharge axis are quantitatively close (as well as in the experiment, there is a movement with acceleration at the phase of growth of the discharge current of the first half-period), and there is a dependence of the average (one half-period) velocity of the shock wave in the gas on the average electrical power, the geometry of the electrodes, the density of the surrounding gas, etc. Thus, in Figure 6, the experimental and calculated graphical dependences of the average velocity of the SW boundary of the MPC discharge on the Ar density are presented. It can be seen that the experiment and calculated results over the entire studied range of characteristics coincide with an accuracy no lower than 20%.

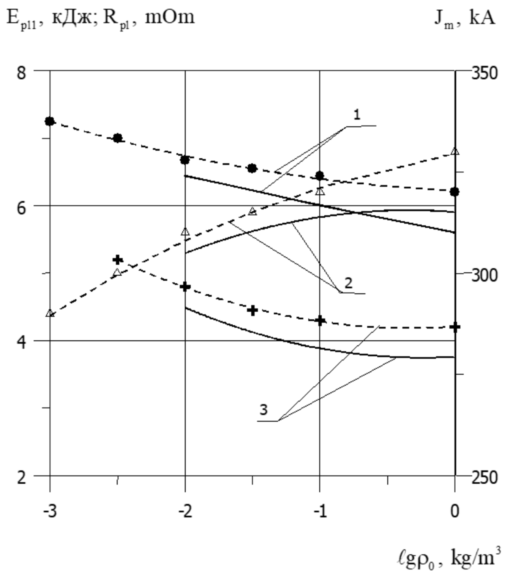

Figure 5. Electrical parameters of MPC discharge (C = 750 µF, U_0 = 5 kV) depending on gas density (argon): 1—E_{pl1}; 2—J_m; 3—R_{pl}, the dotted line corresponds to the experiments [15,16]; the solid line corresponds to the calculation.

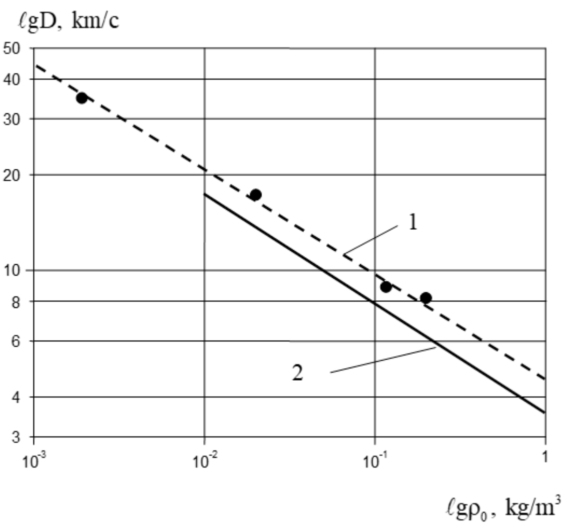

Figure 6. Velocity of the SW boundary of discharge along the MPC-discharge axis (C = 750 µF, U = 5 kV), depending on the density of the surrounding gas (argon): 1—experimental data [15,16]; 2—calculation.

The integral radiative characteristics of MPC discharges are both quantitatively and qualitatively consistent with experimental data [15,16]. Thus, we note that, as in the experiment, the calculations revealed the optimal radiation mode when the integral light output $\eta_{\Sigma m}(A_m)$ is at a maximum. At the same time, the level of the calculated maximum values of light output $\eta_{\Sigma m}$ coincides with the experimental values. Also consistent with the experiment is the fact established by calculation that the type of gas has a rather weak effect on the integral radiative efficiency.

The results of calculations of spectral-brightness characteristics of MPC in general satisfactorily coincide with experiments.

The calculated spectral energy distributions of MPC discharge radiation in gases, depending on the gas density ρ_0, average electrical power P_{el1}, and the type of gas (see Table 2), also correspond to experimental data [15,16].

Table 2. Relative distribution of radiation energy in the MPC discharge spectrum (%).

Gas	Argon			Air
Spectral Interval, eV	MPC Parameters			
	C = 750 μF, U = 5 kV		C = 750 μF, U = 10 kV	C = 750 μF, U = 10 kV
	P = 10^{-1} atm, A_m = 0.6	P = 10^{-2} atm, A_m = 0.8	P = 10^{-2} atm, A_m = 0.85	P = 10^{-2} atm, A_m = 0.85
0.1 ÷ 3.14	20	20	20	40
3.14 ÷ 5.98	30	20	15	50
5.98 ÷ 11.62	50	40	35	10
>11.62	–	20	30	–

At the same time, in the visible range, the "half" duration of the radiation pulse is of the same order as the time of the discharge period and more. The maximum brightness temperature MPC, which occur at times close to the maximum power of the power supply, in calculations and experiments approximately coincide with each other for all of the studied power modes.

As an example, Figure 7 shows the experimental [15,16] and calculated values of the maximum brightness temperature of the MPC in argon and air, depending on the density of the gas (at fixed C = 750 μF, U = 5 kV) and the specific electrical power (at a fixed ambient density).

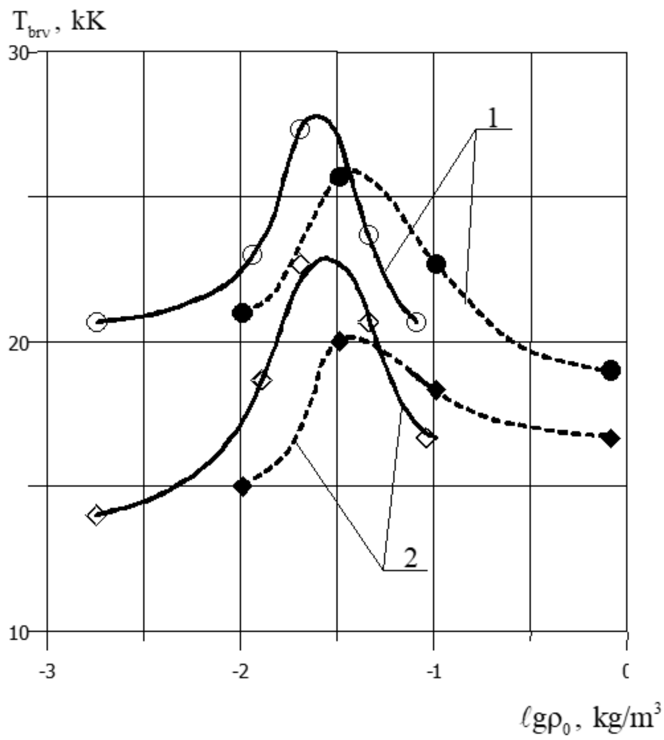

Figure 7. Influence of the gas type and density on brightness temperature in UV region of the spectrum (Δλ = 186 ÷ 200 HM) of MPC discharge with C = 750 μF, U = 5 kV: 1—Ar; 2—air (○, ◊—experiments [15,16]; •, ♦—calculation).

The presented results allow us to report a fairly satisfactory (∼20 ÷ 30%) correspondence of the experimental and calculated data.

6. Conclusions

Herein, a numerical simulation of plasma dynamic magneto plasma compressor discharge in gases was carried out. A numerical simulation of erosive magneto plasma compressors was carried out, which revealed the complex self-consistent nature of energy transfer processes from storage to plasma; the processes of erosive plasma formation, the dynamics of acceleration, and the interaction of light erosive plasma flows between themselves, as well as the surrounding spatial distributions of plasma parameters for ohmic and transient heating modes, were obtained. From the generalized interpolation (according to the results of all calculations), the dependence value on the parameter shows that the role of the ohmic energy dissipation mechanism is significant over almost the entire range of discharge power modes in the magneto plasma compressors and the ambient gas densities.

Further directions of work on the study of the magneto plasma compressor include:

- the possibility of adding new force factors (in addition to the forces of inertia and magnetic field) to increase the efficiency of the magneto plasma compressor;
- establishing the dependence of the main parameters of plasma flows (density, plasma temperature, velocity, energy content) on pressure, type of working gas, and discharge energy;
- optimization of the MPC design and its power supply system in order to reduce its weight and dimensions and increase efficiency.

Author Contributions: Conceptualization, S.V.R.; software, V.V.K.; validation, V.V.K.; writing—original draft preparation, S.V.R. and V.V.K.; writing—review and editing, S.V.R. and A.Y.V.; project administration, S.V.R. All authors have read and agreed to the published version of the manuscript.

Funding: This research received no external funding.

Institutional Review Board Statement: Not applicable.

Informed Consent Statement: Not applicable.

Data Availability Statement: No new data were created or analyzed in this study. Data sharing is not applicable to this article.

Conflicts of Interest: The authors declare no conflict of interest.

References

1. Raizer, Y.P. *Gas Discharge Physics*; Springer: Berlin, Germany, 1991.
2. Stewardson, H.R.; Novac, B.M.; Miran, S.M.; Smith, I.R.; Enache, M.C. A two-stage exploding-foil/plasma erosion opening switch conditioning system. *J. Phys. D Appl. Phys.* **1997**, *30*, 1011. [CrossRef]
3. Giovannini, A.Z.; Barendregt, I.; Haslinde, T.; Hubbs, C.; Abhari, R.S. Self-confined plasma in a magneto-plasma compressor and the influence of an externally imposed magnetic field. *Plasma Sources Sci. Technol.* **2015**, *24*, 025007. [CrossRef]
4. Brovkin, V.G.; Klimov, A.I.; Mashek, I.C.; Pashchina, A.S.; Ryzazansky, N.M.; Vedenin, P.V. Initiation of the plasma jet of the magneto-plasma compressor by the external plasma source. *J. Phys. Conf. Ser.* **2021**, *2100*, 012005. [CrossRef]
5. Zel'dovich, Y.B.; Raizer, Y.P. *Physics of Shock Waves and High-Temperature Hydrodynamic Phenomena*; Dover: Mineola, NY, USA, 2002.
6. Garkusha, I.E.; Chebotarev, V.V.; Herashchenko, S.S.; Makhlaj, V.A.; Kulik, N.V.; Ladygina, M.S.; Marchenko, A.K.; Petrov, Y.V.; Staltsov, V.V.; Shevchuk, P.V.; et al. Novel test-bed facility for PSI issues in fusion reactor conditions on the base of next generation QSPA plasma accelerator. *Nucl. Fusion* **2017**, *57*, 116011. [CrossRef]
7. Grishin, Y.M.; Kozlov, N.P.; Kuzenov, V.V. Singularities of spectral-brightness characteristics of pulsed radiating surface discharges in dense gases. *High Temp.* **1998**, *36*, 169–175.
8. Göksel, B.; Mashek, I.C. First Breakthrough for Future Air-Breathing Magneto-Plasma Propulsion Systems. *J. Phys. Conf. Ser.* **2017**, *825*, 012005. [CrossRef]
9. Kamrukov, A.S.; Kashnikov, G.N.; Kozlov, N.P.; Kondratenko, M.M.; Lebedev, E.F.; Orlov, V.K.; Ostashev, V.E.; Protasov, Y.S.; Semenov, A.M. Experimental investigation of the effectiveness of the matching of a magneto plasma compressor with an explosive magnetohydrodynamic generator. *High Temp.* **1984**, *22*, 313–318.
10. Kuzenov, V.V.; Ryzhkov, S.V. Numerical Simulation of Pulsed Jets of a High-Current Pulsed Surface Discharge. *Comput. Therm. Sci.* **2021**, *13*, 45–56. [CrossRef]
11. Kozlov, A.N. Study of MHD dynamo effect at the outlet from plasma accelerator in the presence of longitudinal magnetic field. *Contrib. Plasma Phys.* **2020**, *60*, e201900174. [CrossRef]

12. Kuzenov, V.V.; Ryzhkov, S.V. The Qualitative and Quantitative Study of Radiation Sources with a Model Configuration of the Electrode System. *Symmetry* **2021**, *13*, 927. [CrossRef]
13. Astashynski, V.M.; Dzahnidze, H.M.; Kostyukevich, E.A.; Kuzmitski, A.M.; Shoronov, P.N.; Shymanski, V.I.; Uglov, V.V. Generation of erosion compression plasma flows in a miniature plasma accelerator and their capability for formation of thin nanostructured coating. *High Temp. Mater. Process.* **2020**, *24*, 99–107. [CrossRef]
14. Kuzenov, V.V.; Ryzhkov, S.V.; Varaksin, A.Y. The Adaptive Composite Block-Structured Grid Calculation of the Gas-Dynamic Characteristics of an Aircraft Moving in a Gas Environment. *Mathematics* **2022**, *10*, 2130. [CrossRef]
15. Kamrukov, A.S.; Kozlov, N.P.; Protasov, Y.S.; Chuvashev, S.N.; Shchepanyuk, T.S. On the influence of hydrodynamic instabilities on the spectral-brightness characteristics of radiating discharges. *Tech. Phys.* **1987**, *57*, 1412–1416.
16. Kamrukov, A.S.; Kozlov, N.P.; Malashchenko, V.A.; Protasov, Y.S. Formation of a plasma focus in a plasma erosion accelerator. III—Radiation properties of the dense plasma focus. *Sov. Phys. Tech. Phys.* **1977**, *22*, 967–974.
17. Vedenov, A.A.; Gladush, G.G. *Physical Processes in Laser Processing of Materials*; Energoatomizdat: Moscow, Russia, 1985.
18. Varaksin, A.Y.; Ryzhkov, S.V. Vortex Flows with Particles and Droplets (A Review). *Symmetry* **2022**, *14*, 2016. [CrossRef]
19. Kuzenov, V.V.; Ryzhkov, S.V.; Varaksin, A.Y. Numerical Modeling of Individual Plasma Dynamic Characteristics of a Light-Erosion MPC Discharge in Gases. *Appl. Sci.* **2022**, *12*, 3610. [CrossRef]
20. Varaksin, A.Y.; Ryzhkov, S.V. Particle-Laden and Droplet-Laden Two-Phase Flows Past Bodies (A Review). *Symmetry* **2023**, *15*, 388. [CrossRef]
21. Varaksin, A.Y.; Ryzhkov, S.V. Turbulence in Two-Phase Flows with Macro-, Micro- and Nanoparticles: A Review. *Symmetry* **2022**, *14*, 2433. [CrossRef]
22. Kuzenov, V.V.; Ryzhkov, S.V.; Varaksin, A.Y. Calculation of heat transfer and drag coefficients for aircraft geometric models. *Appl. Sci.* **2022**, *12*, 11011. [CrossRef]
23. Grishin, Y.M.; Kozlov, N.P.; Kuzenov, V.V. On the degradation of a shock wave in high-current radiating discharges in gases at atmospheric pressure. *Tech. Phys. Lett.* **1998**, *24*, 444–445. [CrossRef]
24. Varaksin, A.Y.; Romash, M.E.; Kopeitsev, V.N. Controlling the behavior of air tornados. *High Temp.* **2009**, *47*, 836–842. [CrossRef]
25. Varaksin, A.Y.; Romash, M.E.; Kopeitsev, V.N. Physical simulation of air tornados: Some dimensionless parameters. *High Temp.* **2011**, *49*, 310–313. [CrossRef]
26. Dyachenko, V.F.; Imshennik, V.S. Two-dimensional magnetohydrodynamic model for the dense plasma focus of a Z pinch. In *Reviews of Plasma Physics*; Leontovich, M.A., Ed.; IOP Publishing: Bristol, UK, 1980; Volume 8, pp. 199–299.
27. Kuzenov, V.V.; Ryzhkov, S.V. Estimation of the neutron generation in the combined magneto-inertial fusion scheme. *Phys. Scripta* **2021**, *96*, 125613. [CrossRef]
28. Olson, G.L. Efficient solution of multi-dimensional flux-limited nonequilibrium radiation diffusion coupled to material conduction with second-order time discretization. *J. Comput. Phys.* **2007**, *226*, 1181. [CrossRef]
29. Braginskii, S.I. Transport processes in plasma. In *Reviews of Plasma Physics*; Leontovich, M.A.I., Ed.; Consultants Bureau: New York, NY, USA, 1965.
30. Surzhikov, S.T. Computing system for solving radiative gasdynamic problems of entry and re-entry space vehicles. In Proceedings of the 1st International Workshop on Radiation of High Temperature Gases in Atmospheric Entry, Lisbon, Portugal, 8–10 October 2003; Volume ESA-533. pp. 111–118.
31. Kuzenov, V.V.; Ryzhkov, S.V.; Shumaev, V.V. Application of Thomas-Fermi model to evaluation of thermodynamic properties of magnetized plasma. *Probl. At. Sci. Technol.* **2015**, *1*, 97–99.
32. Kuzenov, V.V.; Ryzhkov, S.V. Numerical modeling of laser target compression in an external magnetic field. *Math. Model. Comput. Simul.* **2018**, *10*, 255–264. [CrossRef]
33. Volkov, K.N.; Emel'yanov, V.N. *Modelirovanie Krupnykh Vikhrei v Raschetakh Turbulentnykh Techenii (Simulation of Large Eddies in the Calculations of Turbulent Flows)*; Fizmatlit: Moscow, Russia, 2008. (In Russian)
34. Kuzenov, V.V.; Kotov, M.A. Analysis of gas dynamic processes and development of a flow model in a shock hypersonic wind tunnel. *Vestn. Mosk. Gos. Tekh. Univ. N. E. Baumana Ser. Mashinostr.* **2014**, *1*, 3–25. (In Russian)
35. Kuzenov, V.V. Construction of regular adaptive grids in spatial domains with curved boundaries. *Vestn. Mosk. Gos. Tekh. Univ. N. E. Baumana, Ser. Mashinostr.* **2008**, *1*, 3–11. (In Russian)
36. Chetverushkin, B.N. *Mathematical Modeling of Problems in the Dynamics of a Radiating Gas*; Nauka: Moscow, Russia, 1985.
37. Kuzenov, V.V.; Ryzhkov, S.V. Approximate calculation of convective heat transfer near hypersonic aircraft surface. *J. Enhanc. Heat Transf.* **2018**, *25*, 181–193. [CrossRef]
38. Molchanov, A.M. An effective numerical method for simulating chemically and thermally nonequilibrium gas flows. *J. Phys. Conf. Ser.* **2020**, *1683*, 022009. [CrossRef]
39. Formalev, V.F.; Degtyarenko, R.A.; Garibyan, B.A.; Kolesnik, S.A. Modeling heat and mass transfer during periodical spraying of a high-temperature heat-resistant coating. *High Temp.* **2022**, *60* (Suppl. 1), S76–S80. [CrossRef]